Evolution of genotypic and phenotypic diversity in multispecies biofilms

Cristina I. Amador[1], Sofia Zoe Moscovitz[1], Lorrie Maccario[1], Jakob Herschend[1 2], Isabel-Sophie Kramer[1], Hannah Jeckel[3], Vaughn S. Cooper[4], Knut Drescher[3] Thomas R. Neu[5], Mette Burmølle[1] and Henriette L. Røder[1 6 #]

[1]Section of Microbiology, Department of Biology, University of Copenhagen, Copenhagen, Denmark

[2]Present address: Functional Food, Novozymes A/S, 2800, Lyngby, Denmark

[3]Biozentrum, University of Basel, Switzerland

[4]University of Pittsburgh, Pittsburgh, USA

[5]Helmholtz Centre for Environmental Research, Magdeburg, Germany

[6]Pressent address: Section of Microbiology and Fermentation. Department of Food Science, University of Copenhagen. Rolighedsvej 26, 1958 Frederiksberg C, Denmark.

Author correspondence to h.lyng.roeder@food.ku.dk

Running title: Evolution in structured and non-structured multispecies community

Keywords: multispecies, bacterial interactions, biofilm, matrix, adaptive evolution, sporulation

Conflict of interests

The authors declare that no conflicts of interest exist.

Abstract

Interactions occurring in microbial communities can affect the fitness and adaptability of their individual members when facing changing environmental conditions. This study investigated the impact of interspecies interactions in selecting *Bacillus thuringiensis* variants emerging in biofilm and planktonic environments. During evolution experiments, a distinct phenotypic variant of *B. thuringiensis* frequently occurred, despite the presence of other species or culture setup. Remarkably, selection of this variant was significantly favored over its ancestor in biofilm settings and when coexisting with other species co-isolated from a wastewater facility, namely *Pseudomonas defluvii* and *Pseudomonas brenneri*. Interestingly, the evolved phenotype did not show higher biofilm productivity than its ancestor under any condition, while it was indeed reduced in mixed-species biofilms. Such observations aligned with the reduced abundance of TasA, a major biofilm matrix component in *Bacillus* species, and SpoVG, a regulator of sporulation, as revealed by matrix proteomics analysis. Furthermore, the variant showed shorter generation time and a lack of sporulation compared to its ancestor, consistent with mutations in key genes for regulating sporulation. Our results indicate that interspecies interactions within biofilms promote *B. thuringiensis* diversification and alter traits such as biofilm matrix production. Although sporulation is a survival mechanism, this study provides evidence that sporulation does not confer a fitness advantage in *in vitro* biofilm setting, even within mixed cultures, in the absence of severe stress.

Introduction

When encountering new environmental challenges, bacterial populations can adapt through different mechanisms: altering their physiological state (phenotype), i.e. expressing specific traits, acquiring new advantageous mutations (*de novo* genetic variation), or utilizing the pre-existing genetic diversity within the population (standing genetic variation) [1–3]. Besides intraspecific variation, natural communities contain many species that might either constrain adaptation by competing for resources, e.g., via niche exclusion [4] or facilitate adaptation by making new niches available [5, 6]. In biofilms, microbial cells are in close proximity and can influence each other´s phenotypes and evolutionary trajectories through social interactions [7]. Spatial segregation in biofilms increases the frequency of interactions between cells of the same genotype and favors cooperative behaviors but can also support variants outcompeted in unsegregated environments [8–10] and facilitate coexisting populations [11, 12]. Several studies have reported that competitive interactions within biofilms are dominant, including competition for limited space and resources [10, 13–16]. However, there is evidence that competition can subside locally over time, often leading to stable coexistence [17]. Thus, to better understand bacterial adaptation mechanisms in natural environments, investigations of adaptation mechanisms in the presence of spatial structure and multiple species that co-occur in natural communities are crucial.

We have previously described that interspecies interactions can lead to evolved variants that display enhanced mutualism in biofilms [18–20]. The evolution of social interactions in biofilms has been examined for multiple Gram-negative bacteria, including *Pseudomonas spp*. and *Burkholderia cenocepacia* [21–23]. However, comparatively less attention has been dedicated to investigating evolutionary processes in Gram-positive bacteria under mixed-species conditions. Although some studies have explored the adaptive evolution of Gram-positive bacteria in diverse biofilm systems, their focus has primarily been on adaptive genotypes [24–26] or co-culture [20].

In this study, we specifically investigate the influence of cultivation settings and the presence of multiple species on the evolutionary pathways of *Bacillus thuringiensis*, a spore-forming bacterium with

entomopathogenic properties [27]. *B. thuringiensis* was cultivated alone or in combination with *Pseudomonas defluvii* and/or *Pseudomonas brenneri*, co-isolated strains with *B. thuringiensis* from a wastewater facility. In contrast to other studies where cells needed to disperse from biofilms and recolonize new surfaces during the short-term evolution assays, our objective was to identify cells that remained attached within biofilms [20, 28]. We observed that a phenotypic variant of *B. thuringiensis*, that showed reduced Congo red binding, emerged with higher frequency than its ancestor. This phenotype was linked to mutations in sporulation genes and, consequently, lack of sporulation. The evolved phenotype invaded and displaced the ancestral strain under all tested conditions, but co-cultivation with other species and biofilm setup enhanced selection.

Results

Regular emergence of a *B. thuringiensis* morphotype variant after short-term evolution assay

We investigated whether the presence of other species affected selection of new phenotypic variants of *B. thuringiensis* (BT) in biofilm or planktonic conditions. The biofilm condition required cells to attach to polycarbonate slides for 24 hours of growth in either mono-culture, co-culture or multispecies culture, followed by transferring the polycarbonate slide to new media for 8 consecutive cycles. At the end of the experiment, cultures were plated and counted based on distinct colony morphology (Figure 1a).

After 8 days, in all replicate biofilm cultivation experiments, we detected a particular *B. thuringiensis* (BT) phenotypic variant, which we termed "light variant" as it displayed reduced Congo red binding compared to the ancestor (Figure 1b). The population size of BT did not differ among treatments despite the culture condition or composition (mono-culture, two-species culture, or multispecies-culture, Figure 1c). However, the BT light variant independently emerged in each short-term biofilm evolution experiment and displayed significantly higher CFU counts than the ancestral BT strain in all conditions (Figure 1c).

Analogous 8-day evolution experiments in liquid culture showed no significant difference in CFU counts between the ancestral BT and BT light variant in mono-culture conditions. However, in the presence of either *P. brenneri* or *P. defluvii* the BT light variant achieved higher CFU level than the ancestral BT strain, though no significant difference was found within combinations (Figure 1c).

CFU counts were also compared using phenotype as a main factor regardless of the species combination. Detection of the variant phenotype was significantly increased compared to its ancestor regardless of the settings (Welch´s unpaired t-test, $p_{\text{Biofilm}} = 2.84\text{x}10^{-16}$; $p_{\text{Plank}} = 0.0013$ Figure 1c). Together, the results of the short-term evolution experiments in biofilm and planktonic conditions indicate that the BT light variant has a higher fitness in biofilm conditions and in the presence of *P. brenneri* and *P. defluvii*, compared with the ancestral wild-type BT strain.

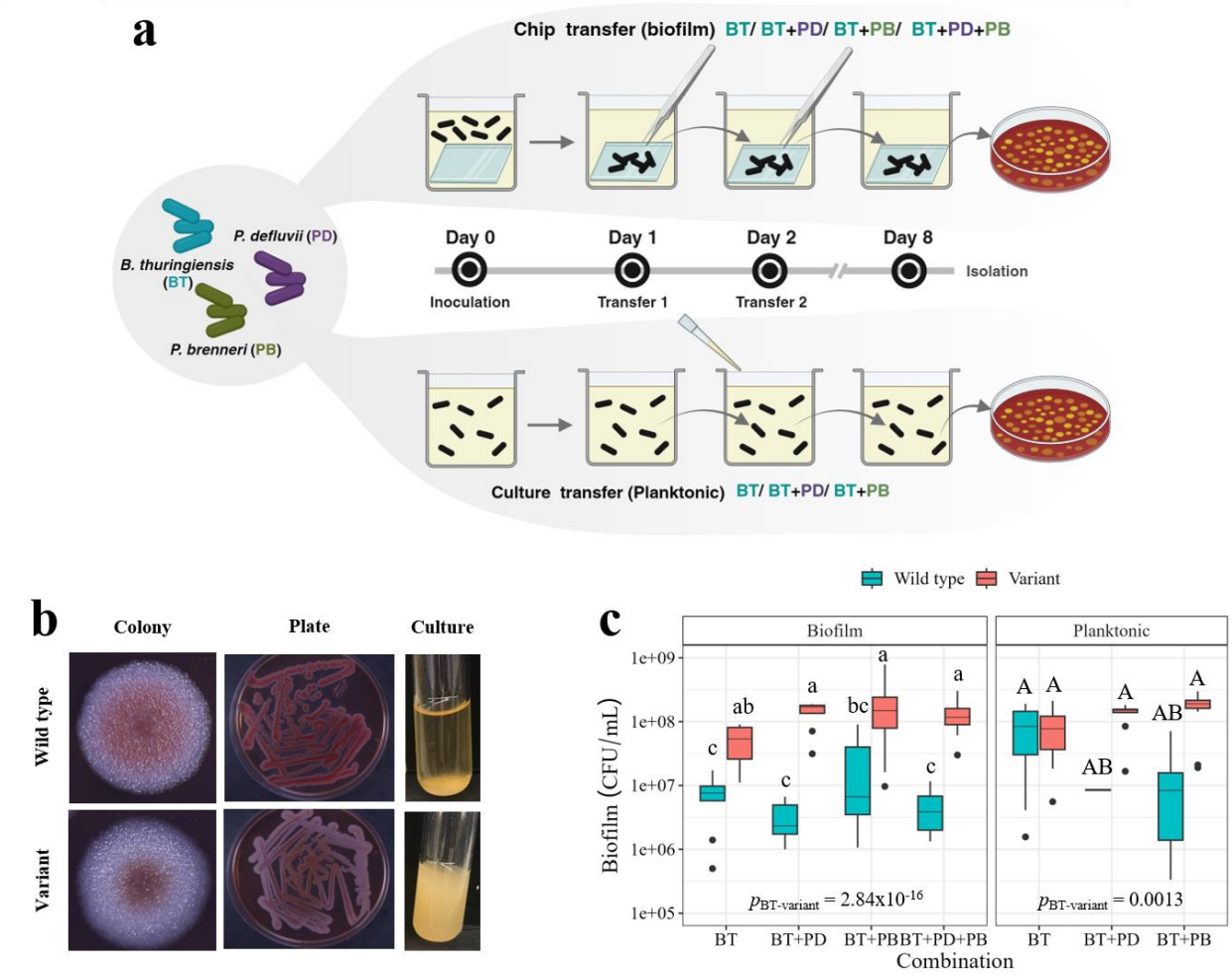

Figure 1. Short-term evolution assay of *Bacillus thuringiensis* in the presence/ absence of *Pseudomonas* species. **(a)** Planktonic/ Biofilm transfer model procedure utilized for the evolution experiment. *B. thurigiensis* (BT) was cultured either individually or together with either or both *P. brenneri* (PB) and *P. defluvii* (PD) in TSB medium in planktonic or biofilm setting and allowed to grow for 24 hours. Then, a polycarbonate chip with attached biofilm was washed thrice and moved to a new well with fresh medium. This was done every day for eight consecutive days, when the biofilms and planktonic samples were plated out and CFU counted. **(b)** Wild-type and variant phenotypes differ in colony morphology (left) and streaks (center) when cultivated on TSB agar supplemented with 40 µg/mL Congo red and 20 µg/mL Coomassie brilliant blue (G). The rightmost panel shows wild type and variant sedimentation phenotypes when the strains are cultivated in liquid TSB. In TSB broth, sedimentation can be observed only for the wild-type strain. **(c)** *B. thuringiensis* cell counts (CFU/mL) of the variant (red) and wild-type (blue) phenotypes in different strain combinations in biofilm (left panel) or planktonic (right panel) setups. Box plots show ≥ 7 biological replicates, represented as individual points, with outliers represented as black points. Dissimilar letters indicate significance per facet (Tukey post-host test, $p < 0.05$).

The selected *B. thuringiensis* variant displayed distinct phenotypic traits compared to its ancestor

We isolated 150 BT light variants from different experiments, and all showed the same phenotypic traits. The ancestral BT and the BT light variant displayed distinct colony morphology but also showed a visibly different phenotype during growth in liquid cultures: the ancestral wild-type BT cells sink to the bottom of the culture in non-shaking conditions, whereas the BT light variant remained in suspension (Figure 1b, right panel).

Besides these phenotypic traits, the BT light variant failed to produce spores compared with the ancestral BT strain, as evidenced by optical microscopy (not shown). Given that the visible phenotypic traits of all 150 isolated light variants were identical, this was tested on four of the selected isolated light variants to test their ability to form spores: V1, V2, V3 and V6. V1 and V2 were isolated from co-cultures with *P. brenneri,* while V3 and V6 were isolated from BT mono-cultures (Table S1). The spore formation ability of BT strains was quantified in planktonic settings over four days and compared to control conditions where only vegetative cells would be able to form colonies. These assays showed that the BT light variants completely lacked spore formation, whereas the ancestral BT strain was able to produce spores despite the incubation time (Figure 2a). Next, we investigated the effect of other species on spore formation in the ancestor. The ability to form spores was assessed in mono-, two-species-, or multispecies biofilm conditions for 24-hour biofilms, however no significant difference was observed between the tested combinations (Figure 2b).

As the variants failed to produce spores, we hypothesized that this might impact their growth rate since sporulation is an energetically costly process for the cell. Thus, growth curves were performed for the BT wild-type and the BT light variants, and different growth parameters were analyzed. We found that the four BT light variants consistently showed a significantly faster doubling time (t_{gen}) and growth rate (r) compared to their ancestor (Table S2). Consequently, the time required to reach half of the maximum culture yield was significantly lower (t_{mid} or ½ k). This suggests that the BT light variants may have a growth advantage compared to wild-type BT when competing for resources with the *Pseudomonas* species,

which could lead to the observed higher CFU counts in mixed-species cultures in our short-term evolution experiments in biofilms and in planktonic cultures.

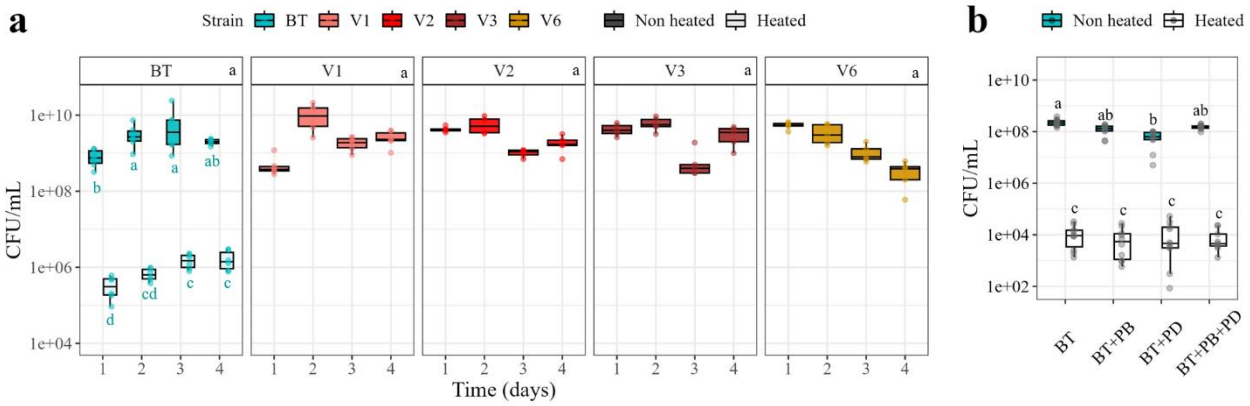

Figure 2. Ability of spore formation for *B. thuringiensis* wild-type or variant phenotypes. (a) Spore forming ability of BT wild-type and variants in a planktonic monocultures after 1, 2, 3 or 4 days incubation, expressed in the same way as a). Box plots show 5 biological replicates, represented as individual points. Outliers are depicted as bigger black points. Dissimilar letters in black indicate significance between strains, or facets ($p < 0.05$, Tukey post-hoc test), while turquoise dissimilar letters denote significant comparisons only within BT (heated vs. non-heated). **(b)** BT wild-type spore formation ability in biofilm settings in different strain combinations, after one-day incubation. Box plots of BT CFU counts in control conditions (vegetative cells, non-heated, blue boxes) and after boiling (germinating spores, heated, white boxes), based on ≥10 biological replicates indicated as independent points, and 3 technical replicates. Dissimilar letters indicate significance ($p < 0.05$, Tukey post-hoc test).

Nutrient reduction selects for higher *B. thuringiensis* diversification in mixed-species biofilms

The presence of other species selected for the BT light variant with higher frequency in full-strength TSB and we thus hypothesized that competition for resources may be a driver of diversification. We reproduced the evolution experiment in a biofilm setting but lowered the nutrients 5-fold (20 % TSB, Figure S1a). CFU counts of BT and variant significantly decreased in 20 % TSB, however the variant exhibited a more pronounced reduction in these conditions (Abundance TSB100 *vs.* TSB20, variant = 13.7-fold, $p = 0$; wt = 2.4-fold, $p = 0.0428$). Unlike 100 % TSB, the wild-type was significantly more abundant in mono-culture, suggesting a fitter wild-type phenotype under reduced nutrient availability in the absence of competing species (Abundance variant vs. wt) = -11-fold, $p = 8.47 \times 10^{-5}$). However, the BT light variant still emerged with higher abundance than the wild-type phenotype when either or both *Pseudomonas*

species were present, although not significant (Abundance variant-wt 20 %: 2.47-fold, $p = 0.0588$, Welch's t-test). Interestingly, comparison of mono-species vs. mixed species within phenotype evidenced significantly enhanced selection of the variant in the presence of either or both *Pseudomonas*, as opposed to significant counter selection of the wild-type phenotype (mixed species vs. monospecies: variant: 9.7 to 19.1-fold; wt: -3.3 to -14.6-fold). These results indicate that the BT light variant has a growth advantage in the presence of other species, even when the nutrients have been reduced 5-fold.

For the CFU counts of *Pseudomonas*, different trends were observed for both strains depending on the media used (Figure S1b-c). PL was negatively affected by the presence of only BT or in the presence of BT and PB in 100 % TSB, but PL abundance did not change significantly in 20 % TSB (Figure S1b; $p_{20\text{-}100} = 0.8537$). PB CFU levels remained stable in full-strength TSB despite the species combination while reduced in 20 % TSB in the presence of BT (Figure S1c). However, no significant difference was observed when comparing PB counts on TSB 100 % and 20 % ($p_{20\text{-}100} = 0.21$, Welch's t-test).

We conclude that, during the evolution experiment, *P. brenneri* abundance significantly decreased in 20% TSB. Since *P. brenneri* enhanced the diversification of *B. thuringiensis* in full-strength TSB, we hypothesize that a lower abundance of *P. brenneri* in 20% TSB may account for the reduced selection of *B. thuringiensis* variants.

The *B. thuringiensis* variant produced less biofilm matrix than its ancestor in mixed species biofilms

An eight-day evolution assay selected for the variant phenotype despite the nutrient concentration and setup (planktonic or biofilm), but its frequency was enhanced in biofilm conditions. In this evolution experiment, our focus was on promoting the retention of cells within the biofilm rather than their dispersal. Consequently, we conducted an investigation to determine if the evolved phenotype exhibited enhanced biofilm formation. We quantified total biofilm formation (cells and matrix) in PC slides after 24 hours using a crystal violet assay but also the contribution of each strain by CFU counts for both the BT wild-type and V1 variant (Figure 3). In mono-culture, biofilm formation (A_{590}) was similar for BT wild-type and variant,

but significantly induced in co-culture or mixed-species cultures despite the BT phenotype (Tukey HSD, $p < 0.0001$) (Figure 3a). Interestingly, species combinations containing the variant phenotype showed significantly decreased biofilm productivity compared to its ancestor ($CV_{wt\text{-}variant}$ = 1.8-fold, $p(_{wt\text{-}variant})$ = 0.02905; Welch´s t-test). However, no significant difference was found when comparing wild-type and variant within each culture condition (co-culture PL, co-culture PB or multispecies). Similar results were observed for V2, V3 and V6 variants, indicating that the source of isolation did not alter their biofilm phenotype (Figure S2a).

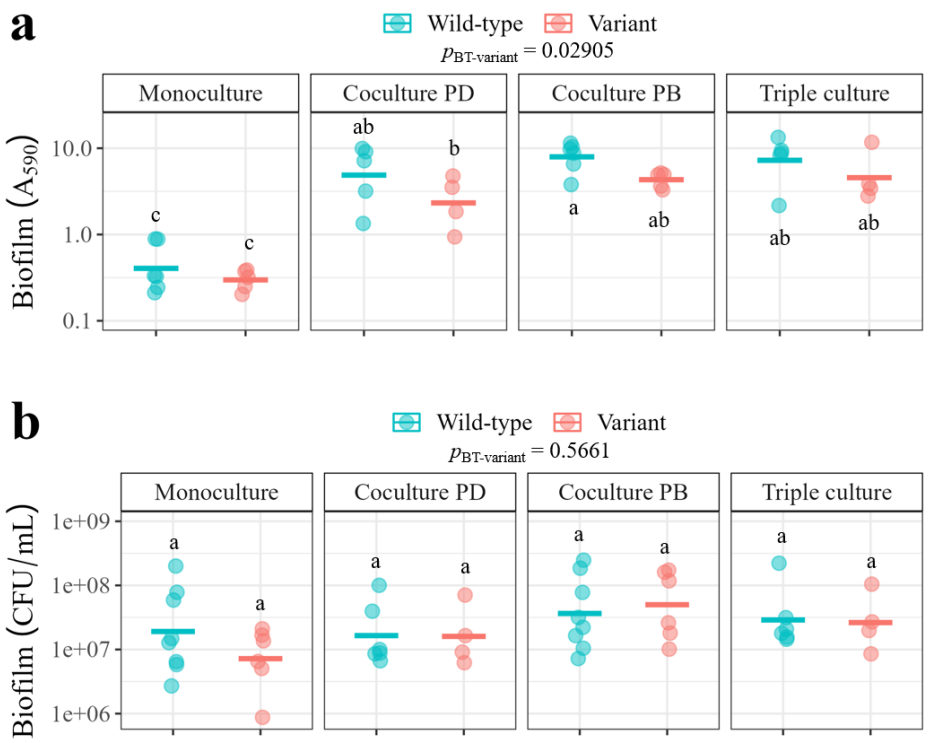

Figure 3. Biofilm formation of *Bacillus thuringiensis* wild-type and V1 variant in mono- or mixed-species cultures in TSB. Wild-type: *B. thuringiensis* wild-type (blue); Variant: *B. thuringiensis* V1 variant (red). Adhesion of wild-type or variant *B. thuringiensis* was measured in monoculture biofilms or in coculture with *P. defluvii* (Coculture PD), *P. brenneri* (Coculture PB) or both *Pseudomonas* (Triple culture). Significance of wild-type vs. variant phenotype is indicated by $p_{BT\text{-}variant}$ (Welch's unpaired two-sample t-test). Dissimilar letters are indicative of significant differences per panel, with $p < 0.05$ (Tukey post-hoc test). **(a)** Total biofilm measured as crystal violet stained biomass (A_{590}) after 24 hours. Data based on ≥ 4 biological replicates and 6 technical replicates. **(b)** *B. thuringiensis* biofilm measured as CFU adhered per mL after 24-hour incubation. Monospecies: cell counts for each species in mono-culture. Data based on ≥ 4 biological replicates, indicated as black dots, and 9 technical.

CFU counts showed no significant difference between wild-type and variant or culture condition (Figure 3b; $p_{phenotype} = 0.563$; $p_{culture} = 0.186$), two-way ANOVA). Comparisons of BT wild-type and variant across all culture conditions (t-test, factor = BT phenotype) resulted in significantly reduced biofilm biomass, but not cell counts, pointing towards differential matrix production/induction. Similar results were observed for the other variants despite the medium strength used (Figure S2b and S2c, 100 % TSB and 20 % TSB, respectively). Furthermore, all variants consistently replicated the results of the evolution experiment in 20 % TSB, with reduced abundance compared to the wild-type in mono-culture conditions ($p_{wt\text{-}variant} = 4.97 \times 10^{-7}$, Welch's t-test). Discrepancies in the biofilm biomass measurements between the CV and CFU methods imply that there could be compensation for adhesion by the *Pseudomonas* species or enhanced production of the biofilm matrix under these specific conditions.

Pseudomonas species showed similar biofilm biomass (A_{590}, crystal violet) in mono-culture, which was significantly induced in co-culture or multispecies (Figure S3a). However, CFU counts were not significantly changed despite the culture condition, except for PL counts in multispecies biofilms with the variant phenotype (Figure S3b PL monospecies vs. multispecies: wt = -2.3-fold, $p = 0.2394$; variant = -9.2-fold, $p = 2.85 \times 10^{-4}$, Tukey's post-hoc test.).

Based on these observations, we can conclude that the variant exhibited comparable colonizing ability to its ancestor in nutrient-rich media. However, there might be a deficiency in its own matrix production or the ability to induce matrix production in the *Pseudomonas* species.

Matrix glycan composition altered by co-cultivation and *B. thuringiensis* adaptive phenotype

BT wild-type and variants showed different phenotypic features and biofilm formation after 24 hours, suggesting differential matrix production in mixed-species biofilms. Thus, we aimed to characterize matrix glycan composition by applying a fluorescent lectin screening in multispecies biofilms (BT+PL+PB), including 78 different lectins binding to carbohydrates of varying nature (Table S3). Binding results were filtered by fluorescence signal (data not shown) and three lectins with strong binding in

multispecies biofilms were selected for further analysis: AAL, WGA and RCA. AAL binds α-fucose-containing polymers, WGA N-acetylglucosamine (GlucNAc) and RCA galactose and N-acetylgalactosamine (Gal/GalNAc) glycans [29]. The binding of such lectins was tested for BT wild-type and variant strains in mono- and dual-species biofilms with PB.

AAL lectin showed differential binding in mono-culture biofilms (Figure 4a). AAL stained BT cells and also some matrix-like structures in BT biofilms, while the variants showed reduced lectin signal. This suggests that glycan composition of the cell wall/surface is distinct in the variants and, thereby, also the AAL binding. Image quantification of lectin binding supported visual observations, with a significant reduction of lectin binding in the variants (Figure 4b). Lectin/biomass ratio –amount of lectin binding per biovolume unit of biofilm biomass– showed a reduced tendency in the variants, though not significant probably due to replicate variation. (Figure 4c). In co-culture with PB, AAL binding was similar despite the BT phenotype, ancestral or variant (Figure S4), suggesting a change of glycan production triggered by interspecies interactions. However, PB also showed AAL binding in mono-culture and, thus, association of lectin signal with the specific matrix producer results cumbersome (Figure S4, BT and PB panels).

Despite the results observed for AAL, RCA lectin did not result in any differential binding of BT or variants in either mono or co-culture with PB. This lectin bound thin filaments are produced by PB, revealing a galactose/N-Acetylgalactosamine polymer network in PB biofilms (Figure S5). WGA bound to BT cell surfaces (Figure S6), likely the cell wall since this lectin binds the sugar GlcNAc, a major component of peptidoglycan [30], but no difference was observed in neither the variants nor mixed-species combinations (data not shown).

B. thuringiensis **protein abundance decreased in response to co-cultivation and genotype**

Biofilm CFU counts as well as crystal violet assays evidenced a biofilm-inducing phenotype in co-cultures of *B. thuringiensis* and *P. brenneri*. BT variants, although more abundant after a short-term evolution assay, displayed reduced biofilm formation and/or matrix production than BT wild-type. Thus, we investigated the influence of interspecies interactions and/or acquired mutations on biofilm matrix proteomes. It is worth

highlighting that we employed a chemical extraction of biofilm matrix as input material for our proteomic experiments and, thus, the number of expected proteins is much lower than for total biofilm samples.

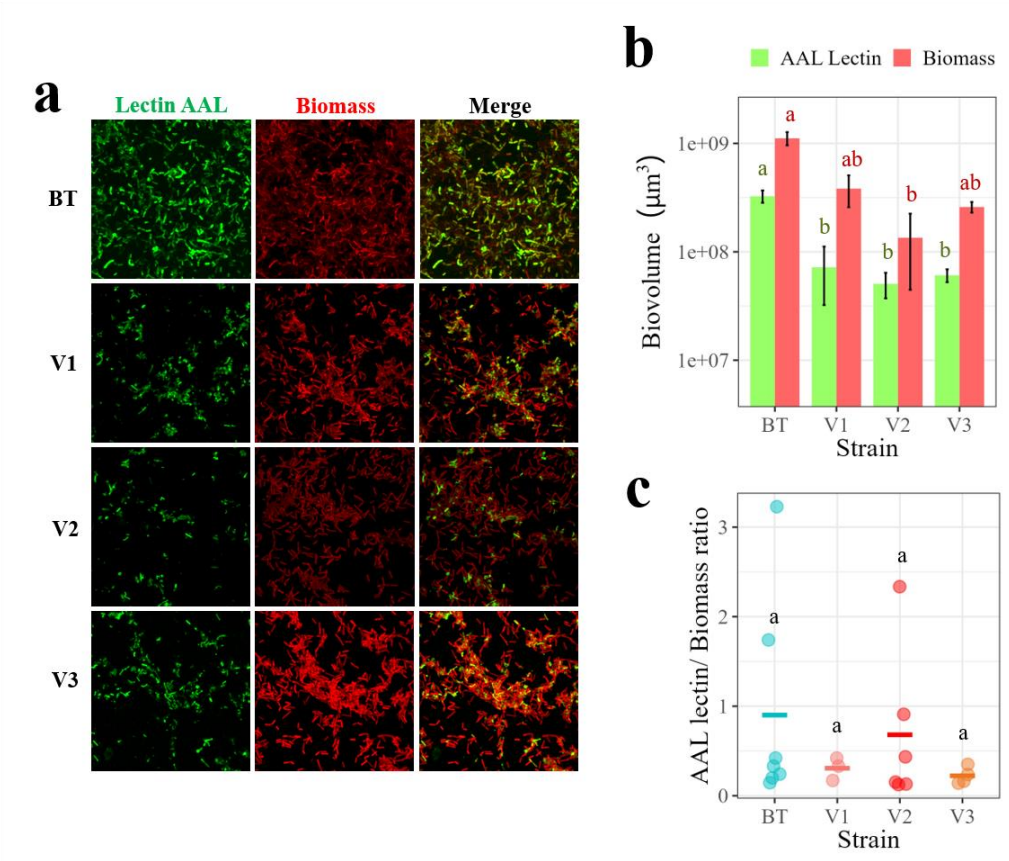

Figure 4. AAL lectin staining of *B. thuringiensis* biofilms of wild-type and variant strains biofilms in monoculture. Dissimilar letters denote significance ($p < 0.05$, Tukey post-hoc test). **(a)** Maximum intensity projection (MIP) images of Z-stacks recorded by confocal laser scanning microscopy for 24-hour biofilms. Biomass: fluorescent images of biofilms stained with the biomass stain Syto60. Lectin AAL: fluorescent images of biofilms stained with the fluorescent lectin AAL-FITC. Merge combined images of biomass and lectin stains. BT: *B. thuringiensis* wt; V1: variant1, V2: variant 2; V3: variant 3; V4: variant 4; PB: *P. brenneri*. The scale of the images is 124 µm across. **(b)** Biofilm biovolume (μm^3) of lectin fluorescence (AAL-FITC, green) and biomass fluorescence (red, Syto60). Biofilm biovolume was calculated using BiofilmQ per channel [31], based on ≥ three biological replicates and two images per replicate. Bars show median values per channel and error bars the standard error of the median. Dissimilar letters denote significant p-value per channel (green = lectin; red = biomass). **(c)** Ratios of lectin biovolume/ biomass biovolume for each strain. Each dot represents a biological replicate and crossbars the median ratio for each strain.

First, we performed a comparative analysis of *B.thuringiensis* proteomes by phenotype, variants or wild-type, in combination with *P. brenneri* (co-culture) or without (mono-culture). Probabilistic principal component analysis (PPCA) evidenced that BT wild-type mono-culture samples were the most distinct

from the rest, clustering together at the right of PC1 (Figure 5a). PC1 variation seemed to be driven by *B. thuringiensis* phenotype (wild-type vs variant), whereas PC2 by cultivation condition (mono-culture vs. co-culture). Variant co-culture or mono-culture samples could not be discriminated, while BT wild-type co-culture samples were grouped in a distinct cluster compared to mono-culture. Interestingly, BT co-culture proteomes overlapped with variant mono- and co-culture proteomes, suggesting a change in protein abundance in the presence of *P. brenneri*. Additionally, different comparisons were made to investigate the impact of such factors on *B. thuringiensis* biofilm proteins: i) mono-culture wild-type vs. variants and ii) co-culture wild-type vs. variants and iii) mono-culture vs. co-culture for each pair (Figure S7b-f). We also inspected iv) *P. brenneri* proteomes comparing mono-culture vs. co-culture per BT strain (Figure S8).

Comparison of BT wild-type vs. variants in mono-culture resulted in 187 proteins detected, 150 uniquely detected in the wild-type (Table S5 and Figure S7b), indicating major downregulation in both variants. Among those, different proteins involved in sporulation or regulated by the Stage 0 sporulation protein, Spo0A, were only detected in the wild-type, consistent with sporulation-defective phenotypes observed in the variants. To discard unique expressions due to detection limits, we calculated the mean and 0.05 percentile of each proteome to use as a cutoff (Table S4 and Figure S8a). However, DivIVA, SpoVG, immune inhibitor A (CDS_04360 and CDS_05099), neutral protease B (CDS_00401) and TasA major biofilm matrix component (CDS_ 04363 and CDS_04365) were still above the expression cutoff in BT wild-type, compared to the variants. Only 20 proteins were common to all three strains (Table S6 and Figure S7b) and 11 significantly changed, related to amino acid and carbohydrate metabolism energy production, among others. We hypothesize that the acquired mutations switch off the expression of multiple genes involved in sporulation, a highly complex and tiered-regulated process. This would be consistent with the faster doubling time observed for the variants, given that fewer proteins, and consequently energy, are required with this expression.

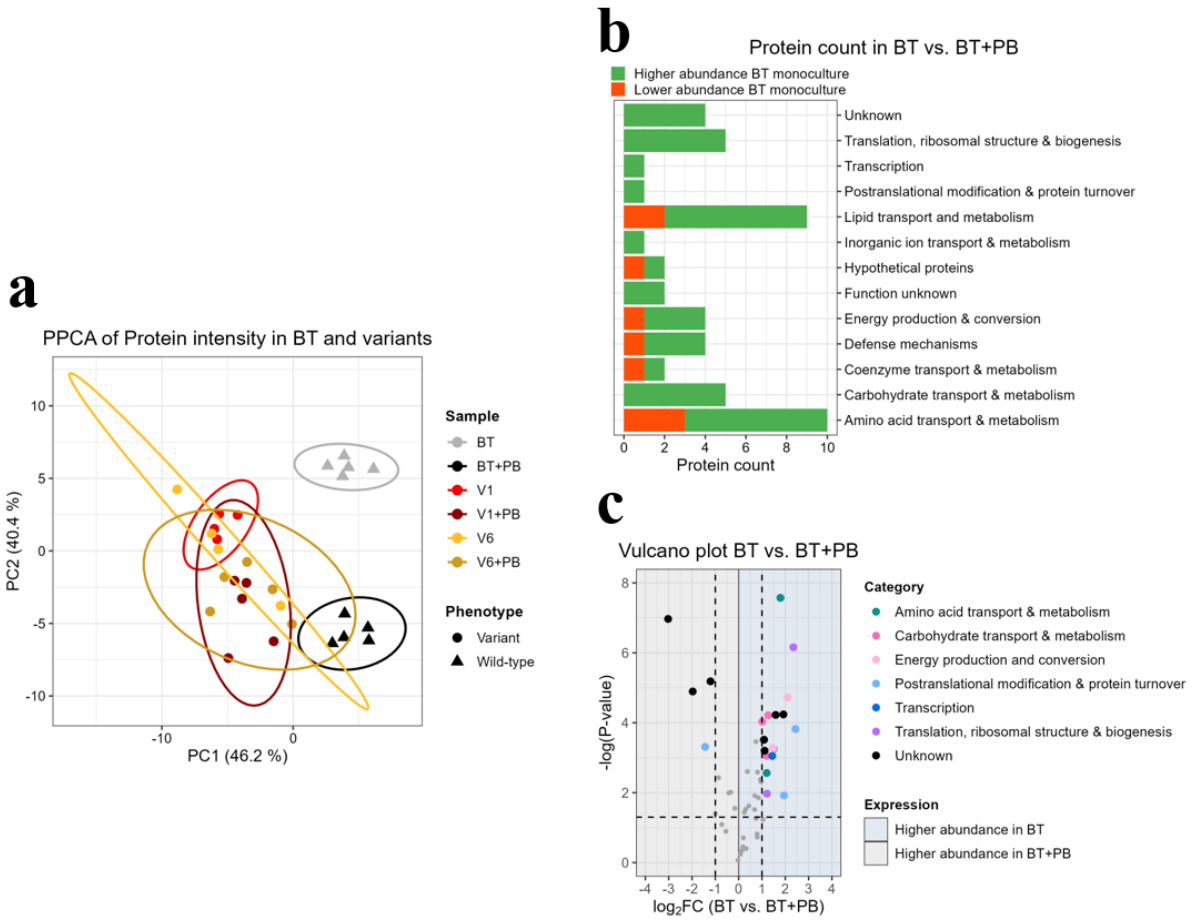

Figure 5. Differential protein abundance in *B. thuringiensis* wild-type *or variants* in mono-culture vs. co-culture biofilms with *P. brenneri*. BT = *B. thuringiensis*; PB = *P. brenneri*; BT_V1 = *B. thurgingiensis* variant 1; BT_V6 = *B. thuringiensis* variant 6. **(a)** Probabilistic PCA plot of all monoculture and co-culture proteomes based on 5 biological replicates. Color indicates the sample type and shape the wild-type (triangles) or variant phenotypes (circles). Ellipses indicate sample group clustering based on the principal components. **(b)** Number of proteins differentially expressed in *B. thuringiensis* wild type mono-culture (BT) vs. co-culture (BT+PB). Green bars indicate proteins with higher abundance in mono-culture while red those decreased in mono-culture and thus, increased in co-culture. Each category role is indicated with a letter code corresponding to the COG classification [32], (A-Z), **(c)** Protein abundance in BT vs BT+PB biofilms. Protein abundance is indicated in the x axis as log2 fold change (log_2FC). Proteins more abundant in co-culture are shown in the grey box (negative values), while more abundant in mono-culture in white (positive values). The y axis indicate –log(P-value). Dashed lines indicate the threshold for significance (y axis) and protein abundance difference (x axis). Proteins with no significant p-value and/ or with difference < 1 and >-1 are depicted as grey dots. Significantly changed proteins are shown as colored points, with each COG category represented by a different color. Categories are the same as in panel (b). Black dots denote not annotated category (ZZ). Analysis was done using data from 5 biological replicates and pairwise comparisons with at least 3 valid values (different to 0) in both co-culture and mono-culture.

The proteomes of BT variants and wild-type were also compared in co-culture. Only a few proteins were detected in the variants, and protein detection in the wild-type was reduced by 70 % compared to the mono-culture proteome. This indicates that *P. brenneri* diminished the disparity between the three proteomes, making them more similar (Figure 4c). In the wild-type co-culture, 15 proteins were uniquely expressed (Table S7), four of which were mentioned earlier (CDS_00401, CDS_04360, CDS_04363, and CDS_04365). Interestingly, these proteins were significantly more abundant in co-cultures (Table S8), suggesting that *P. brenneri* induces their expression, which is dependent on a wild-type phenotype.

Mono-culture vs. co-culture comparisons rendered highly different results depending on the phenotype compared. In the wild-type pairwise analysis, 163 proteins were detected and 111 were only expressed in mono-culture (n = 111), supporting the previous observation that *P. brenneri* reduces abundance of biofilm matrix-associated proteins in *B. thuringiensis.* Fifty proteins were co-expressed in both conditions (Figure 5b) and 50% of which presented significantly different abundance ($p < 0.05$, Welch´s t-test) and log2 fold change greater than 1 (or < -1) (Table S8 and Figures S9a), with amino acid transport and metabolism as the most represented category (Figure S9b). Analysis within the V1 and V6 variants resulted in reduced matrix proteomes, with 15 and 5 proteins detected, respectively, indicating 91-97% downregulation in the variants compared to wild-type proteomes (Tables S9, S10 and Figures S7e-f).

P. brenneri proteomes were subjected to analysis similar to that of BT. A total of 169 proteins were detected and all mono- and co-culture proteomes showed highly similar mean expression and 0.05 quantiles (Table S4 and Figure S8a). Unlike BT results, the presence of other species did not strongly affect the number of proteins detected and 64% of all proteins were shared among all samples (n = 108) (Figure S8b). However, PPCA of all proteomes evidenced a main culture effect, driving PC1, with PB mono-culture samples clustering together and separated from the rest (Figure S8c). Interestingly, seventeen proteins were uniquely expressed in co-culture with BT wild-type (Table S11). However, co-culture samples with BT, V1, or V6 could not be discriminated in the PPCA. Volcano plots of each pairwise comparison supported similar expression patterns of *P. brenneri* in combination with *B. thuringiensis* regardless of the BT

phenotype (Figure S9a). More specifically, co-cultivation resulted in reducedabundance of multiple amino acid transporters in *P. brenneri*, despite *B. thuringiensis* phenotype (Figure S9b).

Based on all proteomics results, it can be concluded that both BT phenotype and co-cultivation impacted protein expression, though with different patterns for the species involved. For *B. thuringiensis*, different proteins involved in sporulation were only detected in the wild-type, but co-cultivation also changed expression significantly and to a similar extent (80% downregulation). However, an abundance of *P. brenneri* proteins was highly influenced by the presence of BT regardless of its phenotype, leading to increased and decreased protein abundance.

B. thuringiensis variants detected mutations in sporulation-related genes

Whole genome sequences of the variants and wild-type revealed mutations in sporulation-related genes in the different variants correlating with the lack of sporulation observed in all the phenotypes. Variants V1, V3 and V6 showed mutations that led to the loss of function of the *spo0A* gene, but of a different nature (Figure 6). The *spo0A* gene encodes a response regulator that, in its phosphorylated active form, activates the transcription of early sporulation genes [33, 34]. Large deletions were found in this region for variants V1 and V3: V1 lacked a 1.5 Kb fragment including most of *spo0A* and CDS0080 genes, while V3 with a 4.5 Kb deletion also covered the *spoIVB* and *recN* genes (Figure 6). V6 only showed a non-synonymous mutation in the *spo0A* gene (C151>T) resulting in a change in the amino acid sequence Q51>stop leading to early termination and, thus, loss of function of Spo0A. These mutations were confirmed by Sanger sequencing using specific primers (data not shown). However, for V2 it was not possible to confirm any clear link to the expected mutations or junction links to the expected phenotype. The mutations found in *spo0A* undoubtedly explain the non-sporulating phenotype for variants V1, V3 and V6 given the central role of *spo0A* and *spoIVB* in the sporulation process.

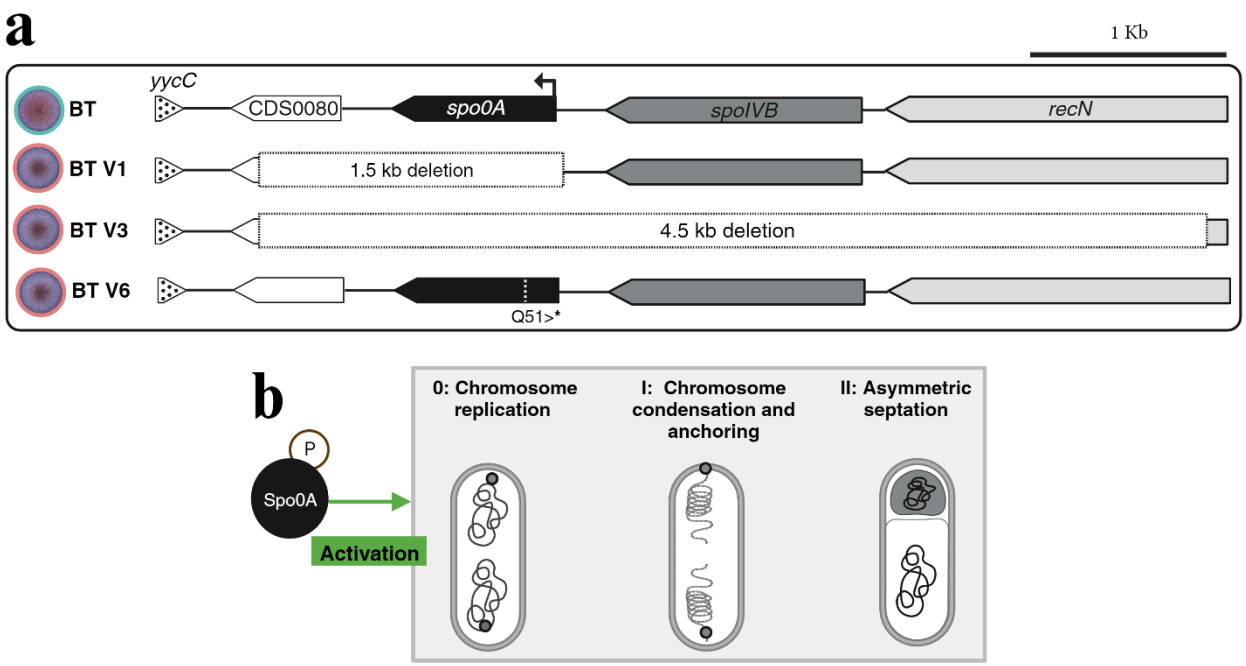

Figure 6. Mutations in *B. thuringiensis* variants compared to wild type and its effect on sporulation pathway. (a) Mutations found in the selected variants (BT Vx, circled pink) compared to their ancestor (BT, circled blue). Dashed boxes indicate large deletions in variants V1 and V3. Q51>* in variant V6 indicates a change in amino acid 51 of the *spo0A* gene from Q to stop codon (*). **(b)** Role of SpoA for activation of the sporulation pathway in *Bacillus* sp. Phosphorylated Spo0A activates transcription of genes involved in sporulation stages 0, I, and II. This figure was created with BioRender.com based on existing literature [35, 36].

Discussion

Microbial interactions can affect fitness and survival of the interacting species and their evolutionary trajectories, for instance, to better exploit available resources, avoid competition, improve mutual dependence or optimize the exchange of nutrients. However, adaptive evolution experiments in multispecies biofilms are still scarce. This study focused on investigating the impact of interspecies interactions and spatial structure on the selection of traits in the Gram-positive bacterium *B. thuringiensis*.

Here, we used short-term evolution assays where *B. thuringiensis, P. defluvii* and *P. brenneri* were cultured alone or combined in planktonic and biofilm settings (Fig. 1a). A novel *B. thurgingiensis* phenotypic variant, which we termed "light variant", emerged in all assays, and displayed a higher abundance than the ancestral wild-type (Fig. 1b-c). We observed that interspecies interactions with *Pseudomonas* species increased the abundance of such a variant, suggesting a fitter phenotype than its ancestor in such conditions. Previous studies of experimental evolution in biofilm settings have reported the emergence of adapted variants in response to other species, however, they usually showed improved biofilm properties compared to their ancestor [18, 20, 37, 38]. Moreover, Lin and collaborators reported the appearance of a fuzzy spreader phenotype of *B. thuringiensis* in a bead-transfer evolution study, where all adapted lineages resulted in enhanced biofilm production compare to its ancestor [26]. In contrast, the *B. thuringiensis* variants selected in this study displayed reduced biofilm productivity, linked to decreased production of biofilm matrix components. Still, the adapted phenotype was favored regardless of the setting (planktonic or biofilm, Fig. 1c) and nutrient availability (Fig. S1). This points towards a gained fitness advantage of the non-sporulating variants over the wild-type, consistent with their faster generation time.

Whole-genome sequencing of the variants linked lack of sporulation with mutations in key genes regulating sporulation genes (Fig. 5). Some of the sequenced isolates of the light variant (V1, V3, V6) harbored mutations in *spo0A* and *spoIVB*, genes with a central role in the sporulation process. The *spo0A* gene encodes a response regulator that, in its phosphorylated active form, activates transcription of early sporulation genes [33, 34]. It has been shown that mutations in *spoIVB* or *spo0A* successfully blocks

sporulation in *Bacillus subtilis.* Consequently, mutations in these genes will result in failure to initiate sporulation or cortex formation and, consequently, explain the non-sporulation phenotype of variants V1 and V3-V6. Interestingly, Spo0A is required for biofilm development in other Bacilli [39–41], while all selected variants of *B. thuringiensis* in this study –lacking Spo0A– conserved biofilm adhesion, despite its reduced productivity compared to the ancestor. These findings indicated that, in the examined conditions, control of biofilm formation in in *B. thuringiensis* deviates from that reported for *B. subtilis* and *B. cereus*.

Irrespective of the particular mutations, all *B. thuringiensis* light variants showed faster generation time than the ancestor (Table S2), non-sporulating phenotype (Figure 2b), and reduced AAL lectin binding (Figure 4), pointing towards a convergent evolutionary pathway for all light variants. Quantification of biofilm biomass by crystal violet assays proved reduced matrix production of the *B. thuringiensis* light variants (Fig. 3a) in mixed culture biofilms suggesting a potential impairment of matrix production, or reduced triggering of matrix production in *Pseudomonas* species. Consistent with this observation, proteomic analysis evidenced unique expression of different matrix proteins in the wild-type. Two TasA/CalY orthologues and SpoVG were expressed in BT wild-type but not in the variants. TasA is a major matrix component in *Bacillus* biofilms and its absence results in significant defects in biofilm and pellicle formation in *B. subtilis* [42, 43] while its paralog is needed for root colonization in *B. cereus* [44]. In *B. thuringiensis*, the TasA-orthologue CalY has been identified as a cell-surface adhesion and described as a major virulence factor and biofilm matrix protein [45]. SpoVG is a regulator of both sporulation and biofilm formation in *B. cereus* 0-9 that activates the levels of Spo0A and, thus, the fate of *B. cereus* cells: biofilm or sporulation [46, 47]. We speculate that the lack of expression of TasA and the biofilm regulatory protein SpoVG could contribute to the differences observed between BT CFU counts and total biofilm biomass for the variant phenotype (CV). Proteomic results also evidenced the unique expression of two metalloproteases only in *B. thuringiensis* wild-type: NprB and InhA (immune inhibitor A). These proteins have been linked with protein recycling during sporulation and are directly or indirectly regulated by Spo0A [33, 48, 49].

From a community perspective, all species were preserved after the 8-day evolution experiment in multispecies combinations (Figure S1), suggesting a stable interaction between the three species. Interestingly, interspecies interactions impacted differently protein abundance depending on the species. We observed that co-cultivation significantly altered the proteome of *B. thuringiensis* but only in the ancestor (Figure 4a). Meanwhile, for *P. brenneri* the presence of BT greatly impacted protein abundance regardless of the phenotype (Figures S8c). An example was a consistent lower abundance of different amino acid transporters in *P. brenneri* co-culture. (Figures S9a-b). We postulate two potential explanations for this observation: competition for resources, specifically amino acids, or utilization or distinct metabolic pathways in co-culture. In co-culture conditions, *P. brenneri* and *B. thuringiensis* might compete for amino acids, leading to a decrease in the availability of certain amino acids in the shared environment, and, thus, amino acid transporters required for uptake of such amino acids. On the other hand, it is also possible that *P. brenneri* reduces amino acids secretion into the environment in response to *B. thuringiensis*, as a strategy of minimizing shared resources with competing species. Alternatively, in mono-culture, *P. brenneri* may rely on its own metabolic pathways or resources that are different from those required in the presence of *B.thuringiensis*. However, when in co-culture, there might be metabolic cooperation or mutualistic interactions between the two species, leading to changes in amino acid utilization and transporter abundance. We have previously reported that cooperative interactions between community members can facilitate metabolic cross-feeding on specific amino acids, though in a different multispecies biofilm model [50, 51]. Additionally, previous studies have shown that coexistence can remain stable over time if they are not exploitable, for instance, altering the pH or secretion of costless by-products to the other species' benefit [52–57]. Given that *B. thuringiensis* doesn´t reduce *P. brenneri* abundance or viceversa, we postulate that a non-exploitable interaction occurs between the variant phenotype and *P. brenneri*, that is, improved growth but not at the cost of the other species.

Biofilm formation and spore production are two different survival strategies of bacteria facing adverse environmental stresses. However, intertwined regulatory pathways between biofilm formation and

sporulation have been proposed for both *B. subtilis* and *B. cereus* [58, 59]. Recent work connects spore formation with biofilm dispersal in *Bacillus subtilis* [60]. When conditions become unfavorable, spores can detach from the biofilm and be carried away by air, water, or other vectors. Dispersed spores can initiate new biofilm formation in different niches, aiding in bacterial survival and colonization. This study used an experimental evolution setup that selected for biofilm-associated cells. In such conditions, we hypothesize that non-sporulating variants would undergo limited passive dispersal and vegetative cells may be forced to stay within the biofilm, dead or alive. Thus, sporulation in such a setting, and in lack of other stresses such as heat or disinfectants, would be dispensable for *B. thuringiensis*.

Our results support that non-sporulating variants can be selected at a higher rate in *in vitro* biofilm setups and in the presence of co-isolated species; thus, spatial structure, diversity and complexity within microbial communities should be considered as drivers of bacterial diversification in such environments.

Methods

Strains and materials

The three bacterial strains *Pseudomonas defluvii* (PL), *Pseudomonas brenneri* (PB) and *Bacillus thuringiensis* (BT) were isolated from water samples taken at a wastewater treatment plant in Kalundborg, Denmark, and genome sequenced earlier. All strains were grown at 24 °C in Tryptic Soy Broth (TSB; 17 g pancreatic digest of casein, 3 g papaic digest of soybean meal, 5 g sodium chloride, 2.5 g dextrose, 2.5 g dibasic potassium phosphate in 1 l distilled water, pH 7.3), supplemented with 1.5 % agar when needed. To distinguish the bacterial strains and/or species variants, 40 µg/ml of Congo Red and 20 µg/ml Coomassie Brilliant Blue G were added to the TSB base.

Short-term evolution assay with spatial structure

Overnight cultures in TSB medium were adjusted to an optical density at 600 nm (OD_{600}) of 0.15 prior to usage. The experiment was conducted in 24-well plates, where each well contained a polycarbonate chip (12 x 12 x 0.78 mm^3) (PC) that served as a surface for establishing the biofilm. In each well, 2 ml of OD_{600} 0.15 cultures were added, either as mono-species culture or mixed-species culture. After 24 hours (h), the floating pellicle was gently removed before the polycarbonate chip was transferred to a new well with fresh media. This was done for 8 days, followed by washing the polycarbonate chip 3 times in 1x phosphate-buffered saline (PBS) and placing it in a 5 ml Eppendorf tube with 2 ml 1x PBS. The biofilm was then removed from the polycarbonate surface and the biofilm structure was homogenized by shaking at 600 rpm for 5 minutes (min). The resulting suspension was then plated on TSB solid medium, complemented with 40 µg/ml Congo Red and 20 µg/ml Coomassie Brilliant Blue with three technical replicates to estimate colony forming units (CFUs) and to screen for new variants with different colony morphology. The same setup was utilized to evaluate interactions between strains and new variants, with growth on polycarbonate chips for 24 h.

Short-term evolution assay without spatial structure

To test selection pressure in conditions not favoring spatial structure, a short-term evolution assay was also performed with well-mixed planktonic cultures. Cultures were adjusted to OD_{600} = 0.15 as before, and 5 ml of this culture was incubated overnight, with shaking at 250 rpm. After 24 h, 5 µl of this culture was transferred to new fresh media. The transfer was repeated for 8 days, followed by plating on TSB solid medium with Congo Red and Coomassie Brilliant Blue, with three technical replicates.

Quantification of biofilm formation

Assessment of the biofilm formation on the polycarbonate surfaces was performed using a modified crystal violet assay [61]. Biofilms were allowed to grow on a polycarbonate surface for 24 h as described above, washed three times in 1x PBS and then transferred to a well of a 24-well plate containing 2 ml of 1 % crystal violet aqueous solution and incubated for 20 min in the dark. Then, polycarbonate chips were carefully removed and rinsed five times in 1x PBS. Crystal violet stained polycarbonate chips were then incubated in 2 ml of 96 % ethanol for 30 min. The biofilm biomass was then quantified as the absorbance of crystal violet at 590 nm (A_{590}). To avoid measurement saturation, samples were diluted in 96% ethanol when A_{590} was higher than 1.

Growth curves in liquid cultures

Cultures of the wild-type and variants were allowed to grow overnight in liquid TSB medium. Then, 1:100 dilutions of the overnight cultures in TSB were prepared, and these cultures were used to inoculate 96-well plates, using 3 biological and 3 technical replicates. Growth was monitored for 24 h at 23 °C with 282 rpm double orbital shaking and OD_{600} readings every 10 min. Growth data was integrated to calculate different growth parameters using the Growthcurver R package [62] to determine the following parameters: t_mid, the point of inflection of the growth curve; K, carrying capacity or maximum size of the population; t_gen, generation time of a strain; r, intrinsic growth rate of a population; sigma, the fit goodness of the model.

Optical microscopy

Liquid cultures of the different strains were incubated for 24 h in TSB, at 24 °C with shaking at 250 rpm. From these 24-h old cultures, 10 µl were pipetted onto a microscope glass slide and a coverslip was applied on top. Samples were observed with an Olympus BH2 optical microscope with 10x and 40x magnification objectives.

Sporulation assay

To compare the sporulation capacity of *Bacillus thuringiensis* and its variants, a sporulation assay was performed. Firstly, the cell concentration in liquid cultures was measured by enumerating CFUs per ml. Next, the culture was heat-shocked at 80 ˚C for 20 min before CFUs were enumerated again. The following calculation was used to estimate the percentage of spores in the culture: colonies per ml after heat shock divided by colonies per ml before heat shock. Furthermore, the sporulation assay was performed for liquid cultures, but also for the biofilms grown on polycarbonate chips, to estimate the number of spores formed in mono-strain cultures and multi-strain cultures.

Biofilm matrix staining with fluorescent lectins

Matrix glycoconjugate characterization in the three species community was performed using 78 different fluorescently labeled lectins (using FITC, AlexaFluor488, or Fluorescein) in combination with confocal laser scanning microscopy (TCS SP5X, Leica Germany, controlled by the software program LAS-AF vers. 2.41) as described previously by Neu and Kuhlicke [63, 64]. The lectins and fluorescent conjugates that were used are listed in Supplementary Table S3. Briefly, biofilms were grown on polycarbonate chips for 24 h, followed by washing three times with 1x PBS, as described above. Staining solutions containing fluorescent lectins were prepared at a concentration of 100 µg/ml (in filter-sterilized ultrapure water). 100 µl was then added to a biofilm on a polycarbonate chip, followed by incubation for 30 min in the dark. Excess staining solution was washed twice with dH_2O before adding SYTO60 to the sample, prior to confocal imaging. Excitation of FITC, AlexaFluor488, and Fluorescein was performed at 488 nm, and the

emission signals were recorded from 500–580 nm. Excitation of SYTO60 was performed at 652 nm and emission was recorded from 665-750 nm. For lectins conjugated to Rhodamine, excitation was done at 525 nm and emission was recorded from 570-650 nm. Image data sets were recorded using 63x NA 0.9 and 63x NA 1.2 objective lenses with a step size of 0.5 µm.

Based on the screening, three lectins: *Aleuria Aurantia* Lectin (AAL), Wheat Germ Agglutinin (WGA) and *Ricinus Communis* Agglutinin (RCA) were chosen for further testing. Here, a dual species combination of *Pseudomonas brenneri* (PB) and *Bacillus thuringiensis* (BT) was used to better estimate the effects between, and on, *Bacillus thuringiensis* and its variant when co-cultured with *Pseudomonas*. Images of AAL-lectin-stained biofilms of BT and variants V1, V2 and V3 were analyzed using the biofilm image analysis software suite BiofilmQ [31]. Biofilm volume (biovolume) was calculated for each fluorescent channel: lectin (FITC channel) and biomass (SYTO60 channel) with a minimum of 6 images per sample (3 biological replicates and 2 images per replicate). Moreover, biovolume ratios (AAL-lectin-stained biovolume divided by the total biovolume) were calculated per biological replicate.

Biofilm matrix proteome measurements

Biofilms were allowed to grow for 24 h in TSB medium on polycarbonate chips as described above, followed by washing 3 times in 1x PBS to remove planktonic cells and biofilm pellicle. Five polycarbonate chips were combined to extract a sufficient amount of biofilm matrix material for proteomics analysis. The biofilm was then resuspended in 5 ml of 1x PBS by shaking at 1000 rpm for 10 min. The biofilm matrix was extracted using the formaldehyde and NaOH extraction method [65, 66]. Briefly, 0.006 V formaldehyde 37 % (30 µl) was added to the biofilm samples and incubated for 1 h at 4 °C while mixing, followed by addition of 0.4 V NaOH 1 N (2 ml) and incubation for 3 h at 4 °C while mixing. Samples were then dialyzed using 3500 MWCO 22 mm SnakeSkin™ Dialysis Tubing (ThermoFisher Scientific) against 2.5 L milliQ water, overnight at 4 °C with stirring. Protein content in dialyzed samples was quantified using the Bio-Rad Protein assay, a modified Bradford assay [67], before freezing with liquid nitrogen. Finally,

extracted biofilm matrix was lyophilized using an ALPHA 1-4 LDplus freeze dryer (Christ, VWR) and kept at -80 °C until sample preparation for proteomics.

For the proteomics sample preparation, digestion, mass spectrometry, and data analysis were conducted as described in Herschend et al. [51] with some modifications, described in the supplementary methods. Reference genomes of *B. thuringiensis*, and *P. brenneri* were prepared as part of a previous study and are available online (NCBI) with IDs JARTVI000000000 and CP122540.1, respectively. The mass spectrometry proteomics raw data and results from analysis by MaxQuant have been deposited to the ProteomeXchange Consortium via the PRIDE [68] partner repository with the dataset identifier PXD046156.

Whole-genome sequencing and analysis of variants

Genomes of *Bacillus thuringiensis* wild-type and variants V1, V2, V3 and V6 (Table S1) were sequenced by extracting the DNA using DNeasy Blood & Tissue Kit (Qiagen) from overnight cultures. The samples were sequenced with short reads using Truseq libraries on the Illumina NovaSeq 6000 and 2x150 cycles (Novogene, UK).

Data was analyzed using breseq (v0.35.0) to call variants using the –p polymorphism flag when analyzing population sequences [69]. As the reference genome, we used the previously constructed hybrid assembly of long and short reads from *B. thuringiensis*, available online (NCBI) with ID JARTVI000000000. Mutations that were detected between our ancestral strain and the reference genome were not considered. The breseq software also predicts new junctions within the genome which may occur due to mobile element insertions, large deletions, structural rearrangements and prophage excision. These analyses were also included. Unfiltered breseq output can be accessed in the supplementary material.

Statistical analysis and visualization

All analysis and plotting was done in RStudio v4.1.1 [70]. Unless otherwise specified, log10 transformed data was fitted to linear models and tested for normality and equal variance. Statistical

significance was tested with a Welch's unpaired t-test when comparing two groups, usually comparing wild-type and variant phenotype (i.e. t-test(CFU~Phenotype)), while ANOVA was applied for more than two groups, using the same parameters as the linear models. A general expression was ANOVA(CFU ~Combination*Phenotype), however the quantitative variable and categorical variables changed depending on the dataset. A Tukey's post-hoc test was performed to consider multiple comparisons when the ANOVA test was significant, unless otherwise specified. A p-value of 0.05 was used as threshold for statistical significance ($p < 0.05$). Compact letter display for multiple comparisons was calculated using R package "multicompView" v0.1-8 [71], while package "ggplot2" v3.4.0 was used for data visualization [72].

Acknowledgments

The authors thank Sara Olsen and Anette Løth for technical assistance, the DTU Proteomics core facility for technical assistance in proteomics sample preparation. Support by Ute Kuhlicke with lectin analysis and confocal laser scanning microscopy is highly appreciated. We thank the Villum Foundation for grants to MB (no. 10098) and HR (no. 34434) and the US Office of Naval Research, for grant N629091812174 to MB, as well as the Swiss National Science Foundation Consolidator Grant TMCG-3_213801 to KD, and the German Bundesministerium für Bildung und Forschung grant TARGET-Biofilms 16GW0245 to KD, funding this work.

Data availability statement

B. thuringiensis and *P. brenneri* genomes are available online at NCBI (https://www.ncbi.nlm.nih.gov/genome/) with the following IDs: JARTVI000000000 and CP122540.1, respectively. The mass spectrometry proteomics raw data and results from analysis by MaxQuant have been deposited to the ProteomeXchange Consortium via the PRIDE [68] partner repository with the dataset identifier PXD046156 (https://www.ebi.ac.uk/pride/archive).

References

1. Agrawal AA. Phenotypic plasticity in the interactions and evolution of species. *Science* 2001; **294**: 321–326.
2. Barrett RDH, Schluter D. Adaptation from standing genetic variation. *Trends Ecol Evol* 2008; **23**: 38–44.
3. Barrick JE, Lenski RE. Genome dynamics during experimental evolution. *Nat Rev Genet 2013 1412* 2013; **14**: 827–839.
4. Scheuerl T, Hopkins M, Nowell RW, Rivett DW, Barraclough TG, Bell T. Bacterial adaptation is constrained in complex communities. *Nat Commun 2020 111* 2020; **11**: 1–8.
5. Calcagno V, Jarne P, Loreau M, Mouquet N, David P. Diversity spurs diversification in ecological communities. *Nat Commun* 2017; **8**.
6. Emerson BC, Kolm N. Species diversity can drive speciation. *Nature* 2005; **434**: 1015–1017.
7. Nadell CD, Xavier JB, Foster KR. The sociobiology of biofilms. *FEMS Microbiol Rev* 2009; **33**: 206–224.
8. Gross K, Cardinale BJ. Does species richness drive community production or vice versa? Reconciling historical and contemporary paradigms in competitive communities. *Am Nat* 2007; **170**: 207–220.
9. Cardinale BJ, Wright JP, Cadotte MW, Carroll IT, Hector A, Srivastava DS, et al. Impacts of plant diversity on biomass production increase through time because of species complementarity. *Proc Natl Acad Sci U S A* 2007; **104**: 18123–18128.
10. Nadell CD, Drescher K, Foster KR. Spatial structure, cooperation and competition in biofilms. *Nat Rev Microbiol 2016 149* 2016; **14**: 589–600.
11. Rainey PB, Travisano M. Adaptive radiation in a heterogeneous environment. *Nat 1998 3946688* 1998; **394**: 69–72.
12. Habets MGJL, Rozen DE, Hoekstra RF, De Visser JAGM. The effect of population structure on the adaptive radiation of microbial populations evolving in spatially structured environments. *Ecol Lett* 2006; **9**: 1041–1048.
13. Foster KR, Bell T. Competition, not cooperation, dominates interactions among culturable microbial species. *Curr Biol* 2012; **22**: 1845–1850.
14. Xavier JB, Foster KR. Cooperation and conflict in microbial biofilms. *Proc Natl Acad Sci U S A* 2007; **104**: 876–881.
15. Rao D, Webb JS, Kjelleberg S. Competitive interactions in mixed-species biofilms containing the marine bacterium Pseudoalteromonas tunicata. *Appl Environ Microbiol* 2005; **71**: 1729–1736.

16. Hibbing ME, Fuqua C, Parsek MR, Peterson SB. Bacterial competition: surviving and thriving in the microbial jungle. *Nat Rev Microbiol* 2010; **8**: 15.
17. Ghoul M, Mitri S. The Ecology and Evolution of Microbial Competition. *Trends Microbiol* 2016; **24**: 833–845.
18. Røder HL, Herschend J, Russel J, Andersen MF, Madsen JS, Sørensen SJ, et al. Enhanced bacterial mutualism through an evolved biofilm phenotype. *ISME J* 2018.
19. Liu W, Jacquiod S, Brejnrod A, Russel J, Burmølle M, Sørensen SJ. Deciphering links between bacterial interactions and spatial organization in multispecies biofilms. *ISME J* 2019; **13**: 3054–3066.
20. Henriksen NNSE, Hansen MF, Kiesewalter HT, Russel J, Nesme J, Foster KR, et al. Biofilm cultivation facilitates coexistence and adaptive evolution in an industrial bacterial community. *NPJ biofilms microbiomes* 2022; **8**.
21. McDonald MJ, Gehrig SM, Meintjes PL, Zhang XX, Rainey PB. Adaptive Divergence in Experimental Populations of Pseudomonas fluorescens. IV. Genetic Constraints Guide Evolutionary Trajectories in a Parallel Adaptive Radiation. *Genetics* 2009; **183**: 1041.
22. Traverse CC, Mayo-Smith LM, Poltak SR, Cooper VS. Tangled bank of experimentally evolved Burkholderia biofilms reflects selection during chronic infections. *Proc Natl Acad Sci U S A* 2013; **110**: E250–E259.
23. Thöming JG, Tomasch J, Preusse M, Koska M, Grahl N, Pohl S, et al. Parallel evolutionary paths to produce more than one Pseudomonas aeruginosa biofilm phenotype. *NPJ Biofilms Microbiomes* 2020; **6**.
24. Leiman SA, Arboleda LC, Spina JS, McLoon AL. SinR is a mutational target for fine-tuning biofilm formation in laboratory-evolved strains of Bacillus subtilis. *BMC Microbiol* 2014; **14**.
25. Dragoš A, Lakshmanan N, Martin M, Horváth B, Maróti G, García CF, et al. Evolution of exploitative interactions during diversification in Bacillus subtilis biofilms. *FEMS Microbiol Ecol* 2018; **94**.
26. Lin Y, Xu X, Maróti G, Strube ML, Kovács ÁT. Adaptation and phenotypic diversification of Bacillus thuringiensis biofilm are accompanied by fuzzy spreader morphotypes. *npj Biofilms Microbiomes 2022 81* 2022; **8**: 1–14.
27. Ehling-Schulz M, Koehler TM, Lereclus D. The Bacillus cereus Group: Bacillus species with Pathogenic Potential. *Microbiol Spectr* 2019; **7**.
28. Poltak SR, Cooper VS. Ecological succession in long-term experimentally evolved biofilms produces synergistic communities. *ISME J* 2011; **5**: 369.
29. Neu TR, Kuhlicke U. Fluorescence Lectin Bar-Coding of Glycoconjugates in the Extracellular

Matrix of Biofilm and Bioaggregate Forming Microorganisms. *Microorganisms* 2017; **5**.

30. Angeles DM, Scheffers DJ. The Cell Wall of Bacillus subtilis. *Curr Issues Mol Biol 2021, Vol 41, Pages 539-596* 2020; **41**: 539–596.

31. Hartmann R, Jeckel H, Jelli E, Singh PK, Vaidya S, Bayer M, et al. Quantitative image analysis of microbial communities with BiofilmQ. *Nat Microbiol 2021 62* 2021; **6**: 151–156.

32. Galperin MY, Wolf YI, Makarova KS, Alvarez RV, Landsman D, Koonin E V. COG database update: focus on microbial diversity, model organisms, and widespread pathogens. *Nucleic Acids Res* 2021; **49**: D274–D281.

33. Fawcett P, Eichenberger P, Losick R, Youngman P. The transcriptional profile of early to middle sporulation in Bacillus subtilis. *Proc Natl Acad Sci U S A* 2000; **97**: 8063–8068.

34. Molle V, Fujita M, Jensen ST, Eichenberger P, González-Pastor JE, Liu JS, et al. The Spo0A regulon of Bacillus subtilis. *Mol Microbiol* 2003; **50**: 1683–1701.

35. Sonenshein AL. Control of sporulation initiation in Bacillus subtilis. *Curr Opin Microbiol* 2000; **3**: 561–566.

36. Tan IS, Ramamurthi KS. Spore formation in Bacillus subtilis. *Environ Microbiol Rep* 2014; **6**: 212.

37. Hansen SK, Rainey PB, Haagensen JAJ, Molin S. Evolution of species interactions in a biofilm community. *Nat 2006 4457127* 2007; **445**: 533–536.

38. Cosetta CM, Niccum B, Kamkari N, Dente M, Podniesinski M, Wolfe BE. Bacterial–fungal interactions promote parallel evolution of global transcriptional regulators in a widespread Staphylococcus species. *ISME J 2023 179* 2023; **17**: 1504–1516.

39. Hamon MA, Lazazzera BA. The sporulation transcription factor Spo0A is required for biofilm development in Bacillus subtilis. *Mol Microbiol* 2001; **42**: 1199–1209.

40. Xu S, Yang N, Zheng S, Yan F, Jiang C, Yu Y, et al. The spo0A-sinI-sinR Regulatory Circuit Plays an Essential Role in Biofilm Formation, Nematicidal Activities, and Plant Protection in Bacillus cereus AR156. *Mol Plant Microbe Interact* 2017; **30**: 603–619.

41. Sharipova M, Rudakova N, Mardanova A, Evtugyn V, Akosah Y, Danilova I, et al. Biofilm Formation by Mutant Strains of Bacilli under Different Stress Conditions. *Microorganisms* 2023; **11**.

42. Romero D, Aguilar C, Losick R, Kolter R. Amyloid fibers provide structural integrity to Bacillus subtilis biofilms. *Proc Natl Acad Sci U S A* 2010; **107**: 2230–2234.

43. Branda SS, Chu F, Kearns DB, Losick R, Kolter R. A major protein component of the Bacillus subtilis biofilm matrix. *Mol Microbiol* 2006; **59**: 1229–1238.

44. Lakshmanan V, Kitto SL, Caplan JL, Hsueh Y-H, Kearns DB, Wu Y-S, et al. Microbe-Associated

Molecular Patterns-Triggered Root Responses Mediate Beneficial Rhizobacterial Recruitment in Arabidopsis 1[C][W][OA]. *Plant Physiol Ò* 2003; **160**: 1642–1661.

45. Candela T, Fagerlund A, Buisson C, Gilois N, Kolstø AB, Økstad OA, et al. CalY is a major virulence factor and a biofilm matrix protein. *Mol Microbiol* 2019; **111**: 1416–1429.

46. Huang Q, Zhang Z, Liu Q, Liu F, Liu Y, Zhang J, et al. SpoVG is an important regulator of sporulation and affects biofilm formation by regulating Spo0A transcription in Bacillus cereus 0–9. *BMC Microbiol* 2021; **21**: 1–17.

47. Lin Y, Briandet R, Kovács ÁT. Bacillus cereus sensu lato biofilm formation and its ecological importance. *Biofilm* . 2022. , **4**

48. Livingston ET, Mursalin MH, Coburn PS, Astley R, Miller FC, Amayem O, et al. Immune inhibitor a metalloproteases contribute to virulence in Bacillus endophthalmitis. *Infect Immun* 2021; **89**.

49. Harwood CR, Kikuchi Y. The ins and outs of Bacillus proteases: activities, functions and commercial significance. *FEMS Microbiol Rev* 2022; **46**: 1–20.

50. Hansen LBS, Ren D, Burmølle M, Sørensen SJ. Distinct gene expression profile of Xanthomonas retroflexus engaged in synergistic multispecies biofilm formation. *ISME J* 2017.

51. Herschend J, Damholt ZBV, Marquard AM, Svensson B, Sørensen SJ, Hägglund P, et al. A meta-proteomics approach to study the interspecies interactions affecting microbial biofilm development in a model community. *Sci Rep* 2017.

52. Ratzke C, Gore J. Modifying and reacting to the environmental pH can drive bacterial interactions. *PLoS Biol* 2018; **16**.

53. Røder HL, Herschend J, Russel J, Andersen MF, Madsen JS, Sørensen SJ, et al. Enhanced bacterial mutualism through an evolved biofilm phenotype. *ISME J* 2018.

54. Herschend J, Koren K, Røder HL, Brejnrod A, Kühl M, Burmølle M. In Vitro Community Synergy between Bacterial Soil Isolates Can Be Facilitated by pH Stabilization of the Environment. *Appl Environ Microbiol* 2018; **84**.

55. Pacheco AR, Segrè D. A multidimensional perspective on microbial interactions. *FEMS Microbiol Lett* 2019; **366**: 125.

56. Aranda-Díaz A, Obadia B, Dodge R, Thomsen T, Hallberg ZF, Güvener ZT, et al. Bacterial interspecies interactions modulate pH-mediated antibiotic tolerance. *Elife* 2020; **9**.

57. Fritts RK, McCully AL, McKinlay JB. Extracellular Metabolism Sets the Table for Microbial Cross-Feeding. *Microbiol Mol Biol Rev* 2021; **85**.

58. Vishnoi M, Narula J, Devi SN, Dao HA, Igoshin OA, Fujita M. Triggering sporulation in Bacillus subtilis with artificial two-component systems reveals the importance of proper Spo0A activation

dynamics. *Mol Microbiol* 2013; **90**: 181–194.

59. Huang Y, Flint SH, Palmer JS. Bacillus cereus spores and toxins – The potential role of biofilms. *Food Microbiol* 2020; **90**: 103493.

60. Nishikawa M, Kobayashi K. Calcium Prevents Biofilm Dispersion in Bacillus subtilis. *J Bacteriol* 2021; **203**.

61. O'Toole G, Kolter R. Initiation of biofilm formation in Pseudomonas fluorescens WCS365 proceeds via multiple, convergent signalling pathways: a genetic analysis. *Mol Microbiol* 1998; **28**: 449–461.

62. Sprouffske K, Wagner A. Growthcurver: An R package for obtaining interpretable metrics from microbial growth curves. *BMC Bioinformatics* 2016; **17**: 1–4.

63. Neu T, Kuhlicke U. Fluorescence Lectin Bar-Coding of Glycoconjugates in the Extracellular Matrix of Biofilm and Bioaggregate Forming Microorganisms. *Microorganisms* 2017.

64. Neu TR, Kuhlicke U. Matrix glycoconjugate characterization in multispecies biofilms and bioaggregates from the environment by means of fluorescently-labeled lectins. *Front Microbiol* 2022; **13**.

65. Liu H, Fang HHP. Extraction of extracellular polymeric substances (EPS) of sludges. *J Biotechnol* 2002; **95**: 249–256.

66. Pan X, Liu J, Zhang D, Chen XI, Li L, Song W, et al. A comparison of five extraction methods for extracellular polymeric substances (EPS) from biofilm by using three-dimensional excitation-emission matrix (3DEEM) fluorescence spectroscopy. *undefined* 2010; **36**: 111–116.

67. Bradford MM. A rapid and sensitive method for the quantitation of microgram quantities of protein utilizing the principle of protein-dye binding. *Anal Biochem* 1976; **72**: 248–254.

68. Perez-Riverol Y, Bai J, Bandla C, García-Seisdedos D, Hewapathirana S, Kamatchinathan S, et al. The PRIDE database resources in 2022: a hub for mass spectrometry-based proteomics evidences. *Nucleic Acids Res* 2022; **50**: D543–D552.

69. Deatherage DE, Barrick JE. Identification of mutations in laboratory-evolved microbes from next-generation sequencing data using breseq. *Methods Mol Biol* 2014; **1151**: 165–188.

70. Team. RStudio: Integrated Development for R. *Rstudio, BMC* 2021.

71. Piepho HP. An Algorithm for a Letter-Based Representation of All-Pairwise Comparisons. *http://dx.doi.org/101198/1061860043515* 2012; **13**: 456–466.

72. Wickham H. ggplot2: Elegant Graphics for Data Analysis. 2016. Springer-Verlag, New York.

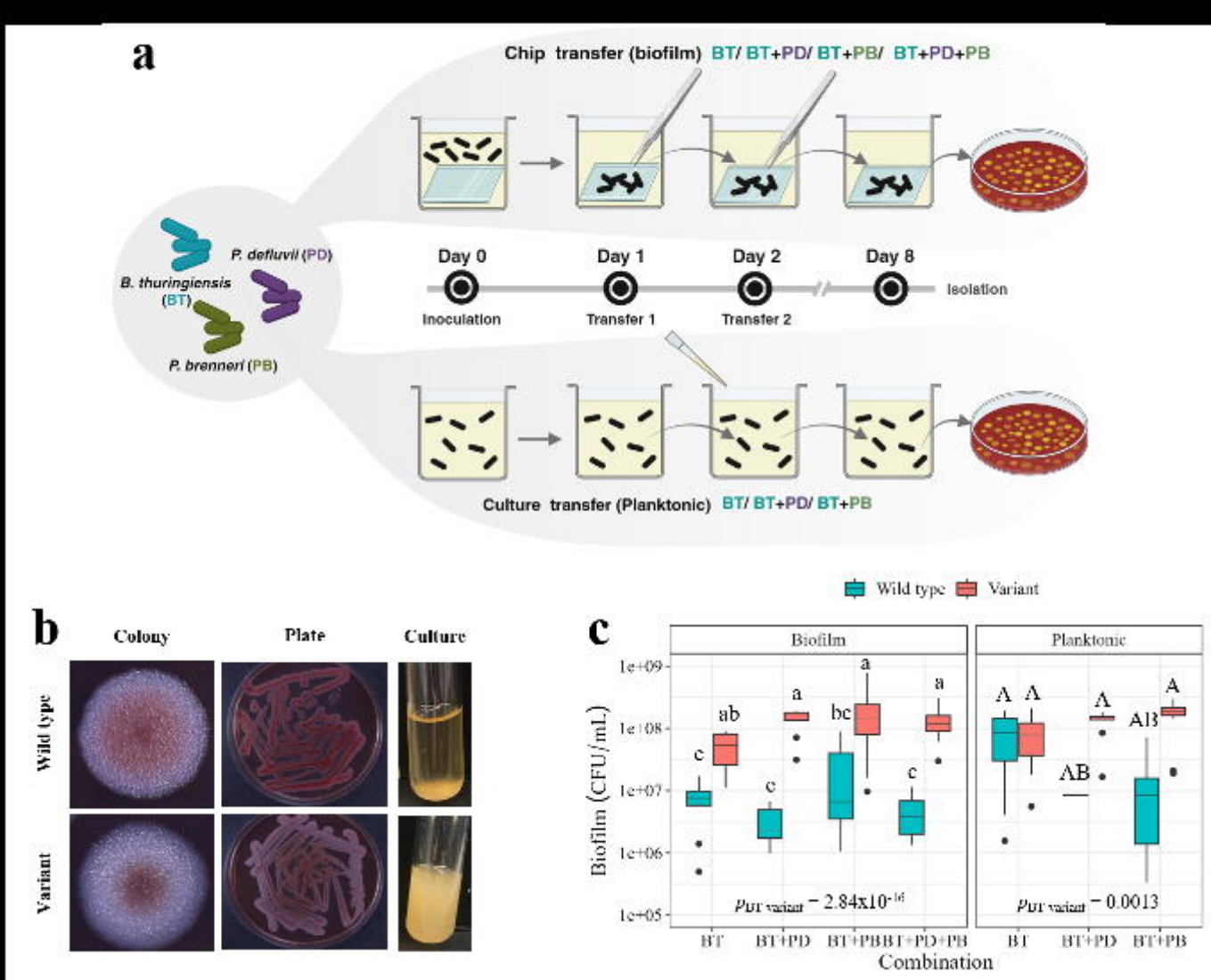
a
Chip transfer (biofilm) BT/ BT+PD/ BT+PB/ BT+PD+PB
P. defluvii (PD)
B. thuringiensis (BT)
P. brenneri (PB)
Day 0
Day 1
Day 2
Day 8
Isolation
Inoculation
Transfer 1
Transfer 2
Culture transfer (Planktonic) BT/ BT+PD/ BT+PB
b
Colony
Plate
Culture
Wild type
Variant
c
Wild type
Variant
Biofilm
Planktonic
Biofilm (CFU/mL)
1e+09
1e+08
1e+07
1e+06
1e+05
$p_{BT\ variant} = 2.84x10^{-16}$
$p_{BT\ variant} = 0.0013$
BT
BT+PD
BT+PB
BT+PD+PB
Combination

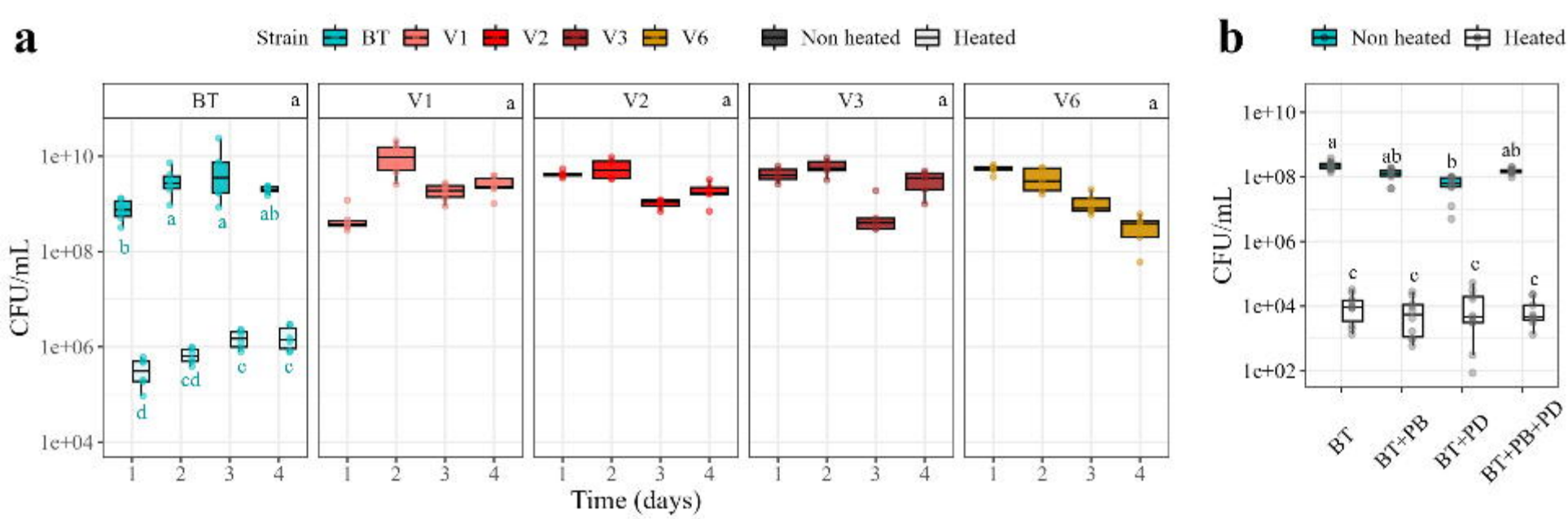
a
Strain
BT
V1
V2
V3
V6
Non heated
Heated
CFU/mL
1e+10
1e+08
1e+06
1e+04
Time (days)
b
1e+02
BT
BT+PB
BT+PD
BT+PB+PD

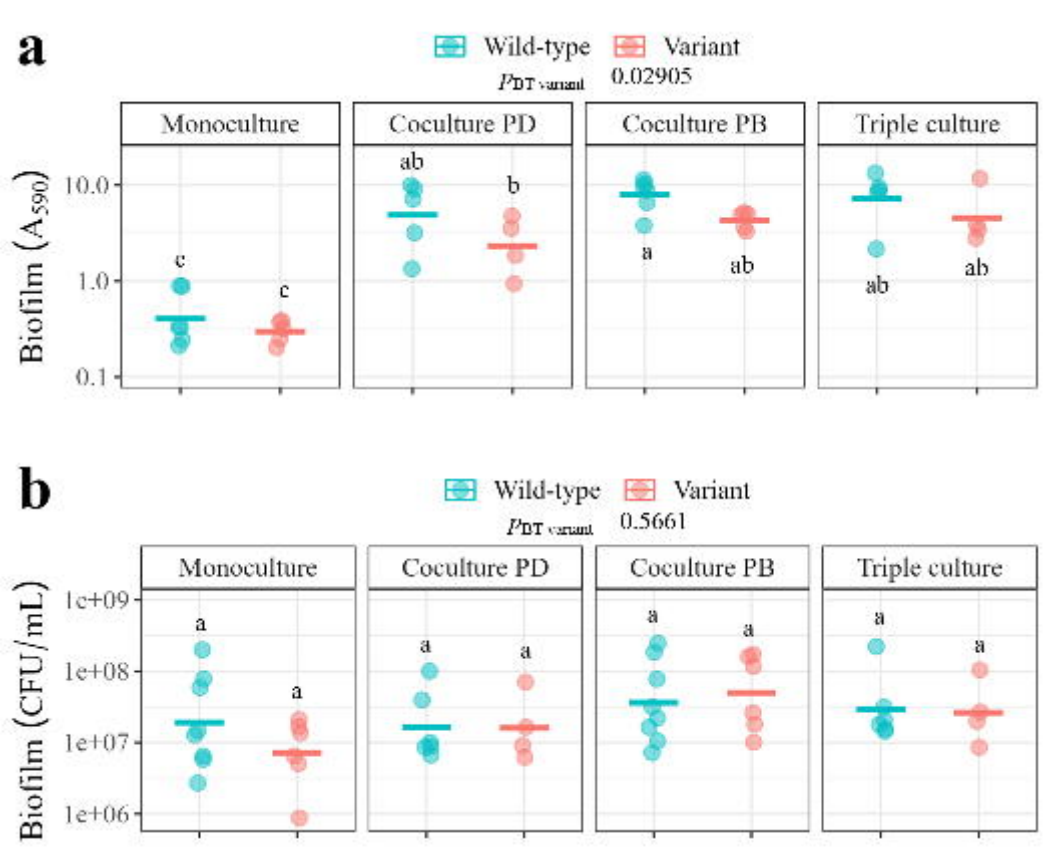
a
Wild-type
Variant
$P_{DT\ variant}$ 0.02905
Monoculture
Coculture PD
Coculture PB
Triple culture
Biofilm (A_{590})
10.0
1.0
0.1
c
c
ab
b
a
ab
ab
ab
b
Wild-type
Variant
$P_{DT\ variant}$ 0.5661
Monoculture
Coculture PD
Coculture PB
Triple culture
Biofilm (CFU/mL)
1e+09
1e+08
1e+07
1e+06
a
a
a
a
a
a
a
a

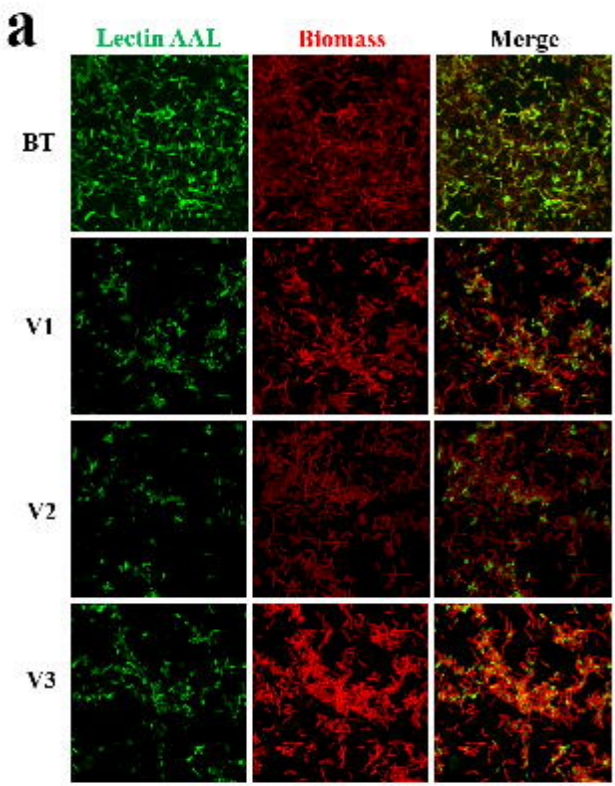
a
Lectin AAL
Biomass
Merge
BT
V1
V2
V3

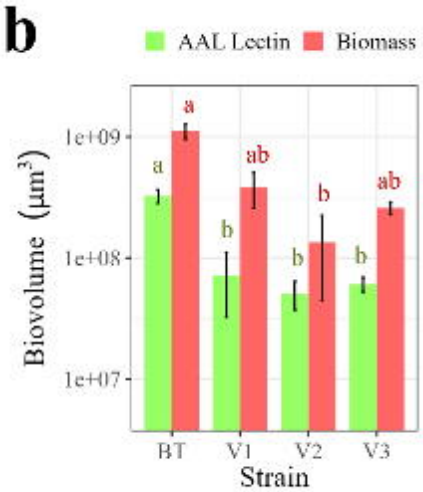
b
AAL Lectin
Biomass
Biovolume (μm³)
1e+09
1e+08
1e+07
a
a
b
ab
b
b
b
ab
BT
V1
V2
V3
Strain

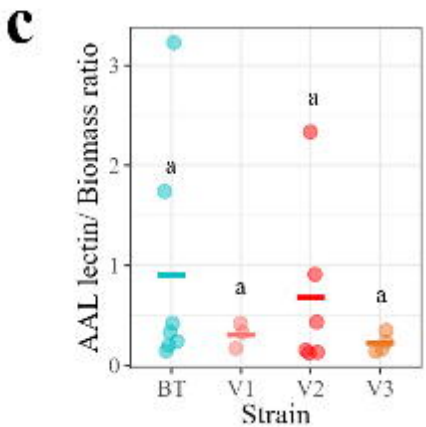
c
AAL lectin/ Biomass ratio
3
2
1
0
a
a
a
a
BT
V1
V2
V3
Strain

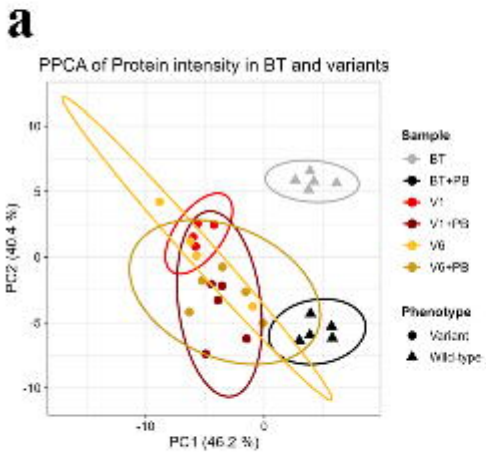
a
PPCA of Protein intensity in BT and variants
PC2 (40.4 %)
PC1 (46.2 %)
Sample
BT
BT+PB
V1
V1+PB
V6
V6+PB
Phenotype
Variant
Wild-type

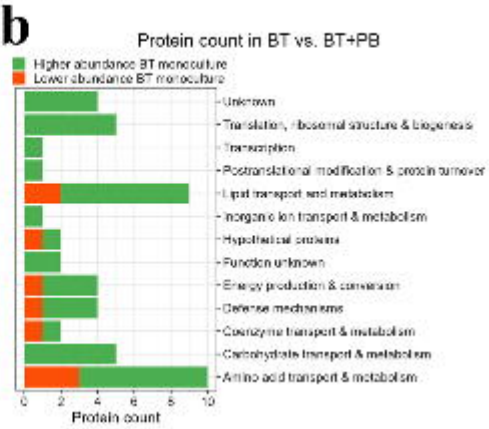
b
Protein count in BT vs. BT+PB
Higher abundance BT monoculture
Lower abundance BT monoculture
Unknown
Translation, ribosomal structure & biogenesis
Transcription
Postranslational modification & protein turnover
Lipid transport and metabolism
Inorganic ion transport & metabolism
Hypothetical proteins
Function unknown
Energy production & conversion
Defense mechanisms
Coenzyme transport & metabolism
Carbohydrate transport & metabolism
Amino acid transport & metabolism
Protein count

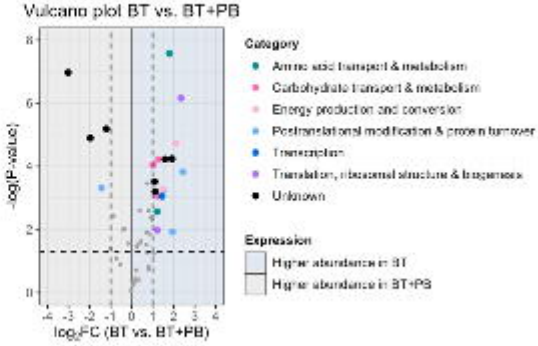
c
Vulcano plot BT vs. BT+PB
-log(P-value)
log2FC (BT vs. BT+PB)
Category
Amino acid transport & metabolism
Carbohydrate transport & metabolism
Energy production and conversion
Postranslational modification & protein turnover
Transcription
Translation, ribosomal structure & biogenesis
Unknown
Expression
Higher abundance in BT
Higher abundance in BT+PB

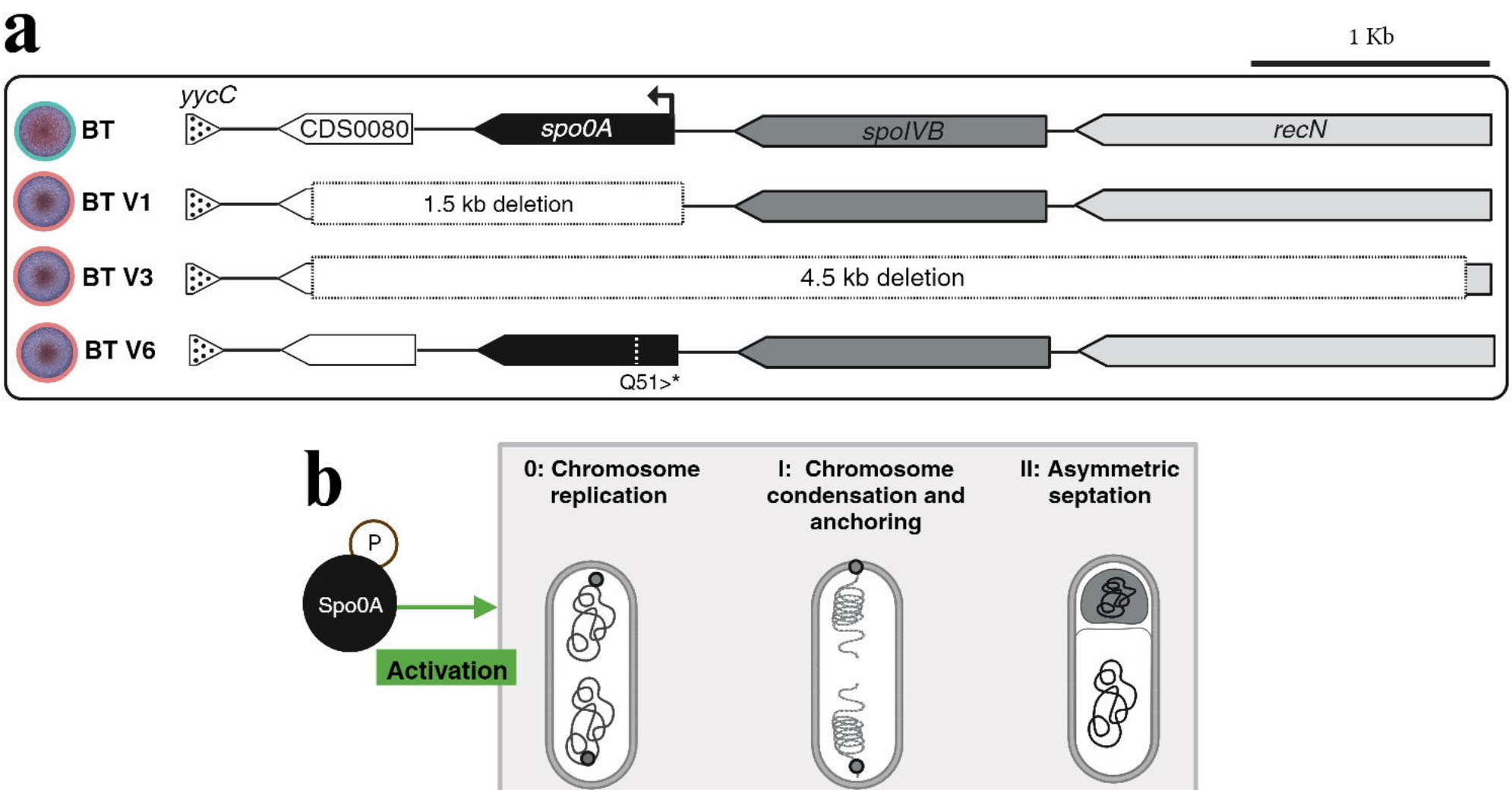
a
1 Kb
BT
yycC
CDS0080
spo0A
spoIVB
recN
BT V1
1.5 kb deletion
BT V3
4.5 kb deletion
BT V6
Q51>*
b
P
Spo0A
Activation
0: Chromosome replication
I: Chromosome condensation and anchoring
II: Asymmetric septation